PAPER • **OPEN ACCESS**

3D-ElectroZip touch: multi-directional haptic feedback with electro-ribbon zipping actuators

To cite this article: Yuhan Pan *et al* 2024 *Smart Mater. Struct.* **33** 085030

OPEN ACCESS
IOP Publishing
Smart Materials and Structures
Smart Mater. Struct. **33** (2024) 085030 (10pp)
https://doi.org/10.1088/1361-665X/ad61a3

3D-ElectroZip touch: multi-directional haptic feedback with electro-ribbon zipping actuators

Yuhan Pan[1], **Ningzhe Hou**[1], **Wenjie Sun**[1,2] **and Majid Taghavi**[1,*]

[1] Department of Bioengineering, Imperial College London, London, United Kingdom
[2] School of Mechanical and Precision Instrument Engineering, Xi'an University of Technology, Xi'an, People's Republic of China

E-mail: m.taghavi@imperial.ac.uk

Received 6 June 2023, revised 26 April 2024
Accepted for publication 10 July 2024
Published 22 July 2024

Abstract

This paper introduces the 3D-ElectroZip Touch, a multi-directional force feedback device developed using dielectrophoretic liquid zipping actuation. The device is designed to stimulate the sense of normal and shear forces by moving in vertical and multiple horizontal directions. Its performance, including displacement, force, and actuation time has been characterized under input voltages from 6 kV to 9 kV, demonstrating a displacement range of 5–11 mm, force range of 0.05 N to 0.22 N, power output ranges from 0.08 W to 0.077 W, and maximum energy efficiency of 72%. The 3D-ElectroZip Touch shows a quick response to the input signal, moving its contact panel by 1.1 mm in 70 ms (36.5% of human reaction time) at 9 kV. Comparing its basic characteristics with the skin sensitivity and the lightweight, compliance, and scalability of the 3D-ElectroZip Touch technology show its high potential to be exploited in tactile displays and wearable haptic feedback devices.

Keywords: haptic, multi-directional, soft actuator, dielectrophoretic liquid zipping, electro-ribbon

1. Introduction

The skin, the most expansive organ in the human body, is densely innervated with tactile sensory nerves, converting thermal, mechanical, and chemical environmental stimuli into sensory data. The haptic perceptual system, comparable in complexity, processes even more information than visual and auditory systems. Consequently, the creation of a haptic device delivering dynamic tactile information and haptic feedback to human skin can significantly enhance human information access. A long-standing engineering goal has been to realize haptic devices that simulate the feeling of natural touch [1]. The potential of haptic devices in human–computer interaction has been explored as they enable operators to receive realistic feedback on interaction information in remote or virtual operations through haptic stimulation [2]. Today, haptic devices are being used in many different fields, such as virtual reality [3], teleoperation [4], and medical applications [5]. For instance, in Robot-assisted minimally invasive surgery, a haptic device could enable surgeons to tangibly interact with a patient's body, thereby improving surgical precision and safety. However, the technology is still in its early stages, with most devices limited

* Author to whom any correspondence should be addressed.

to kinesthetic force feedback and lacking genuine tactile perception [6].

A haptic device delivering precise information for such applications must satisfy several essential factors, including controllability, responsiveness, compliance, and the device's size and weight. In response, various actuation mechanisms have been developed using different active material combinations. Arguably, pneumatic actuators are the most widely utilized soft actuation method, enabling simple and practical mechanisms [7, 8] Wu *et al* demonstrated a pneumatic Braille display [9] and Agharese *et al* designed wearable, restricted-aperture pneumatics haptic feedback device [10]. However, pneumatic actuators have some inherent limitations, including the need for significant energy resources, bulky and noisy control units, and potential pressure loss during sudden volume changes [1] which can significantly affect the pneumatic actuator's controllability. Moreover, these actuators typically exhibit relatively low actuation frequency, which can impair information accuracy.

Gels exhibit mechanical deformations based on different chemical principles, many of which have been used in constructing soft actuators. Miruchna *et al* reported a haptic device [11] using a thermoresponsive hydrogel that can transition from soft to stiff with temperature changes, thus enabling haptic information conveyance through viscoelasticity alterations. In addition to tactile feedback, hydrogel thermocouples have been utilized to provide kinesthetic haptic feedback by restricting finger motion in a glove, to create a realistic and immersive tactile experience for the user [12]. While gel-based haptic devices provide excellent flexibility, the gel must be maintained in a semi-liquid state, which can make the resulting devices mechanically sensitive. Furthermore, gel actuators generally result in relatively low bandwidths [1]. Furthermore, semi-active actuators using electrorheological [13] or magnetorheological [14–16] have also been used to provide haptic force feedback. Instead of applying force directly to the skin, these devices can alter the material's stiffness to vary the tactile sensation.

Another widely used haptic actuation method is electromagnetic actuation. These actuators [17–19] harness the electromagnetic forces to generate mechanical work. For instance, Kastor *et al* [20] designed a high-fidelity compact haptic feedback device with a magnetically driven, fabric-reinforced elastic membrane. Similarly, Guo *et al* [21] introduced a programmable electromagnetic-actuated soft tactile device, distinguished by its ability to maintain the pit depth of tactile pixels without any energy consumption. Moreover, Kim *et al* [22] adopted a flip-latch structured electromagnetic actuator to realize a braille display for portable devices with low power consumption. Furthermore, Hosseini *et al* [23] proposed a low-cost kinesthetic haptic feedback glove that utilizes an electromagnetic motor based on a twisted string actuation system. It is important to note that while these traditional electromagnetic actuators can achieve high bandwidth, dynamic movement ranges, and precise controllability, their reliance on a permanent magnet partially embedded in the soft material thus limits their applications in wearables.

One of the major limitations of most haptic stimulation materials is their limited degree of freedom. Since they employ only one-DOF (Degrees of Freedom) actuation [2], users are often only able to interact with virtual objects in a limited way. Recent research has been placing greater emphasis on multi-degree-of-freedom haptic feedback systems to address the needs of progressively complex working conditions [24–26]. Mintchev *et al* [27] applied origami design principles to realize three degrees of freedom force feedback for human-robot interactions. Zhao *et al* [28] propose an innovative wearable haptic communication device that utilizes four dielectric elastomer linear actuators arranged in a two-by-two array, featuring a broad bandwidth (10 Hz up to 200 Hz). Furthermore, Leroy *et al* [29] employed electrostatic force to develop a versatile haptic device with multifaceted motion capabilities. During actuation, dielectric liquid is displaced into a stretchable region, creating a bump that facilitates the transmission of haptic information. Despite its rapid and efficient response, this flexible device relies on small oil-filled pouches, which are susceptible to bursting under pressure, limiting its scalability in denser configurations.

Such electrostatic actuators in general may be considered as the most suitable actuation mechanism for multi-modal haptic feedback devices since they can generate stimulation in multiple directions. The intensity of the force can be precisely controlled with the input voltage and their power consumption is low. Electrostatic haptic devices have also been demonstrated in different configurations [30, 31] where squeezing the electroactive polymer between two electrodes by coulomb forces produces tapping-like stimulation under altering voltages. Although these devices can achieve only vertical motion as limited by their structures, they have shown great potential for using electrostatic force in haptic stimulation devices.

Here we introduce a new type of scalable electro-active haptic stimulation technology which can provide multi-directional motion aiming to extend the range of haptic device applications in various fields. We developed this haptic unit based on the dielectrophoretic liquid zipping (DLZ) actuation concept [32]. DLZ allows for large and fast displacement between two insulated electrodes, harnessing giant amplification in electrostatic force. We demonstrate a novel structure that employs DLZ actuation for both vertical and horizontal motions in different directions to give the user tapping and sliding feedback. The developed multi-directional haptic unit (3D-ElectroZip Touch) can move in seven directions with its displacement being precisely controlled by the input voltage.

2. Device design

3D-ElectroZip Touch consists of three pairs of ribbon electrodes, separated by two PVC insulation layers. Figure 1(a) shows a pair of ribbon electrodes where the insulated bottom

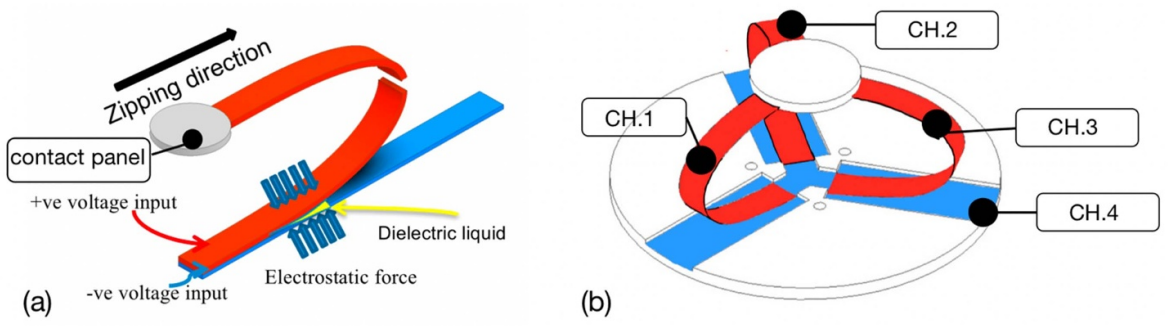

Figure 1. 3D-ElectroZip touch: (a) a configuration of the actuation module. (b) An initial design of the whole device using three pairs of electrodes.

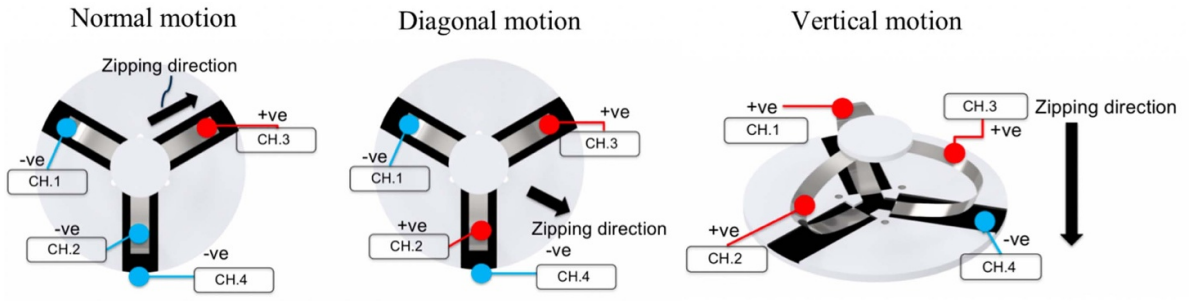

Figure 2. Three motion modes under different input conditions.

electrode (blue) is fixed on the substrate and the top electrode (red) is bent to form a semicircle shape. The top ribbon electrode is aligned longitudinally with the bottom ribbon electrode and clamped to this insulated electrode. We call this clamping area as the zipping point. When the electrodes are oppositely charged, a strong electric field is generated at the zipping point, and an electrostatic force is exerted to zip the electrodes together. The addition of a bead of dielectric liquid to the zipping point significantly amplifies the generated force, as demonstrated in the electro-ribbon actuators [32]. As the electrodes zip together, the liquid bead, driven by the dielectrophoretic force, allows for the concentrated and amplified electrostatic zipping force to move along the ribbons. Depending on the movement restrictions applied to the other end of the top electrode (the contact panel in figure 1(a)), the top electrode may move along the bottom electrode to achieve lateral motion or be pulled down as a result of the change in the top electrode's curvature.

The 3D-ElectroZip Touch haptic unit's design, featuring three pairs of zipping electrodes, is displayed in figure 1(b). The three movable electrodes are directly connected to a thin plastic disc (the contact panel) on top of the device. They can be individually charged to interact with the opposite fixed electrode, driving the contact panel in different directions. The contact panel is part of the device that directly contacts the human body, transmitting the simulated force.

As shown in figure 1(b), each of these three movable electrodes is connected to a high-voltage channel (CH.1, CH2, and CH.3) whose output can be controlled independently. All the bottom electrodes are connected to a single high-voltage channel (CH.4). The electrostatic Maxwell stress is applied along the oppositely charged ribbons (between CH.4 and one of the other three channels) and thus enables the movement of the contact panel forward along the ribbons, and downward. The integration of three independent pairs of actuators generates three different displacement patterns as shown in figure 2. Normal motion pattern is achieved when only one pair is oppositely charged; diagonal motion pattern is achieved when any two pairs are actuated at the same time; vertical motion is achieved when all pairs are actuated together.

3. Methods

3.1. Structural components and fabrication process

Figure 3 presents a deconstructed view of the 3D-ElectroZip Touch device, which comprises five principal components: the contact panel, moving electrodes, fixing ring, fixed electrodes, and the base. The height of the entire touch prototype is 40 mm, and it is attached to a square base with side lengths of 80 mm. The length of one side of the fixed electrode is 24 mm, with adjacent fixed electrodes positioned 51 mm apart.

(1) **Contact panel**: The contact panel is a three-layer circular disc with a 2 cm diameter, approximately the same size as a human fingertip, and a thickness of 1.5 mm. The bottom layer serves to connect the moving electrodes, while the

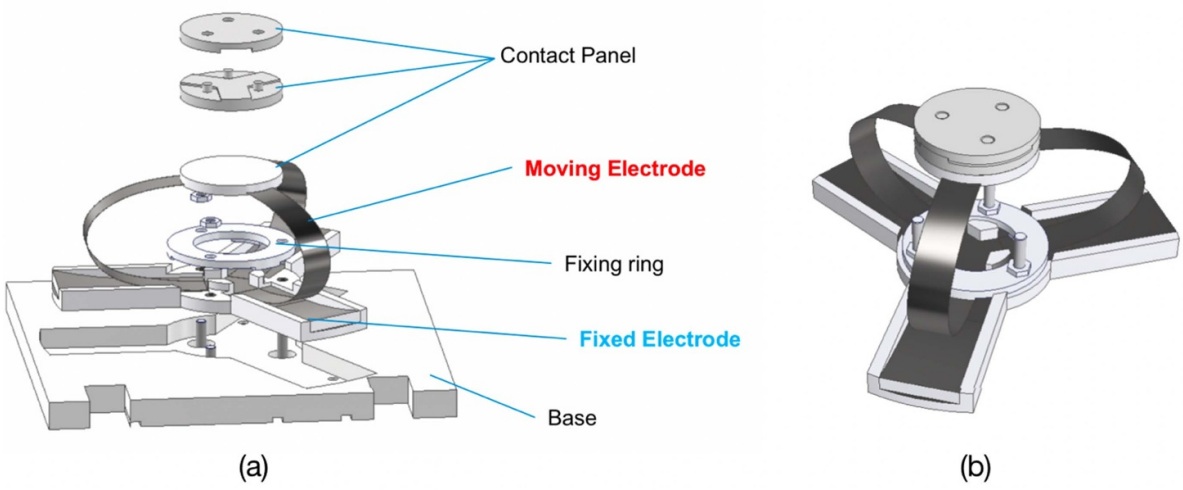

Figure 3. (a) An assembly drawing showing all components of the 3D-ElectroZip Touch. (b) Isometric view of the 3D-ElectroZip Touch device.

middle layer is adhered to the bottom layers to secure the electrodes. The top layer, designed to be the only part of the device in direct contact with users, is affixed to the middle layer via insertion, facilitating easy replacement. This top layer can be replaced with various materials with different surface roughness and shapes to enhance the tactile sensations provided by the device. All these layers are fabricated using Anycubic photo-curable resin (Anycubic, HK), to ensure the contact panel is non-conductive and safe to touch when the electrodes are charged.

(2) **Movable electrode**: The choice of materials with suitable mechanical properties is an essential part of movable electrode fabrication and largely determines the overall performance of this device. After testing different combinations of materials, carbon steel 1.1274 (C-Stahl gehartet 1.1274, h + s, Germany) with a thickness of 0.03 mm has been used. This material easily bends, forming an optimal initial zipping angle. Its mechanical stiffness counteracts the electrostatic zipping force without hindering the operation of the 3D-ElectroZip Touch and reverts the device back to its original position when voltage is turned OFF. The size of the movable electrodes is $65 \times 5 \times 0.03$ mm, cut out by a Circut machine (Cricut maker, Cricut, Inc., USA). One end of the movable electrodes was glued onto the notches over the bottom layer of the contact panel, and the other end was firmly clamped to the base by the fixing ring together with the fixed electrode. Figure 4 illustrates the whole fabrication process of the movable electrodes.

(3) **Fixed electrode**: Copper tape (Kraftex, Germany) was used as the conductive material for the fixed electrodes because the copper foil is ductile and can be easily cut into the relatively complex shape required for the fixed electrode. The copper foil is then encapsulated by one layer of 0.13 mm PVC tape (AT7 PVC Electrical Insulation Tape, ADVANCE, UK) from both sides to provide durable electrical insulation.

(4) **Fixing ring and base**: The fixing ring and base are 3d-printed using PLA material. The fixing ring is designed to clamp the electrodes onto the base and to create the initial zipping point between movable and fixed electrodes. The base is designed to be slightly curved to retain the dielectric liquid droplet (silicon oil) during operation, thus preventing any loss of liquid that could alter the consistency of the characterization results.

3.2. Experiment setup and data analysis

To characterize ElectroZip Touch, its displacement and force were measured at different input voltages. Power output and energy conversion efficiency have been calculated accordingly. Below are setups and data processing methods for obtaining different types of measurements.

(1) **Displacement measurement**: Displacements were recorded in the vertical direction and six horizontal directions (60 degrees apart from each other). The device is set up as shown in figure 5(a). Top layer of the contact panel is replaced by a hexagonal cap, the displacement of the device in each direction is measured by positioning the laser sensor (LG-GD500, Keyence, Japan) directly to the hexagonal cap in the corresponding directions of the device.

(2) **Force measurement**: The setup shown in figure 5(b) measures the magnitude of the force generated by the device in two modes of motions (normal motion and diagonal motion). A spring holder was made to replace the top layer of the contact panel, and then a spring with stiffness $k = 0.11$ N mm^{-1} was connected between the spring holder and a fixed hook. At the end of the spring, a piece of cardboard is fixed with a specifically designed clip. When the device is activated, the generated net force pulls the spring to reach a stable state. The magnitude of the generated net force is found by Hook's law, $F = kx$, where k is the known stiffness of the spring and x is the extension of the spring, obtained by measuring the corresponding displacement of the cardboard. To measure the normal force, we connected the contact panel to a force sensor

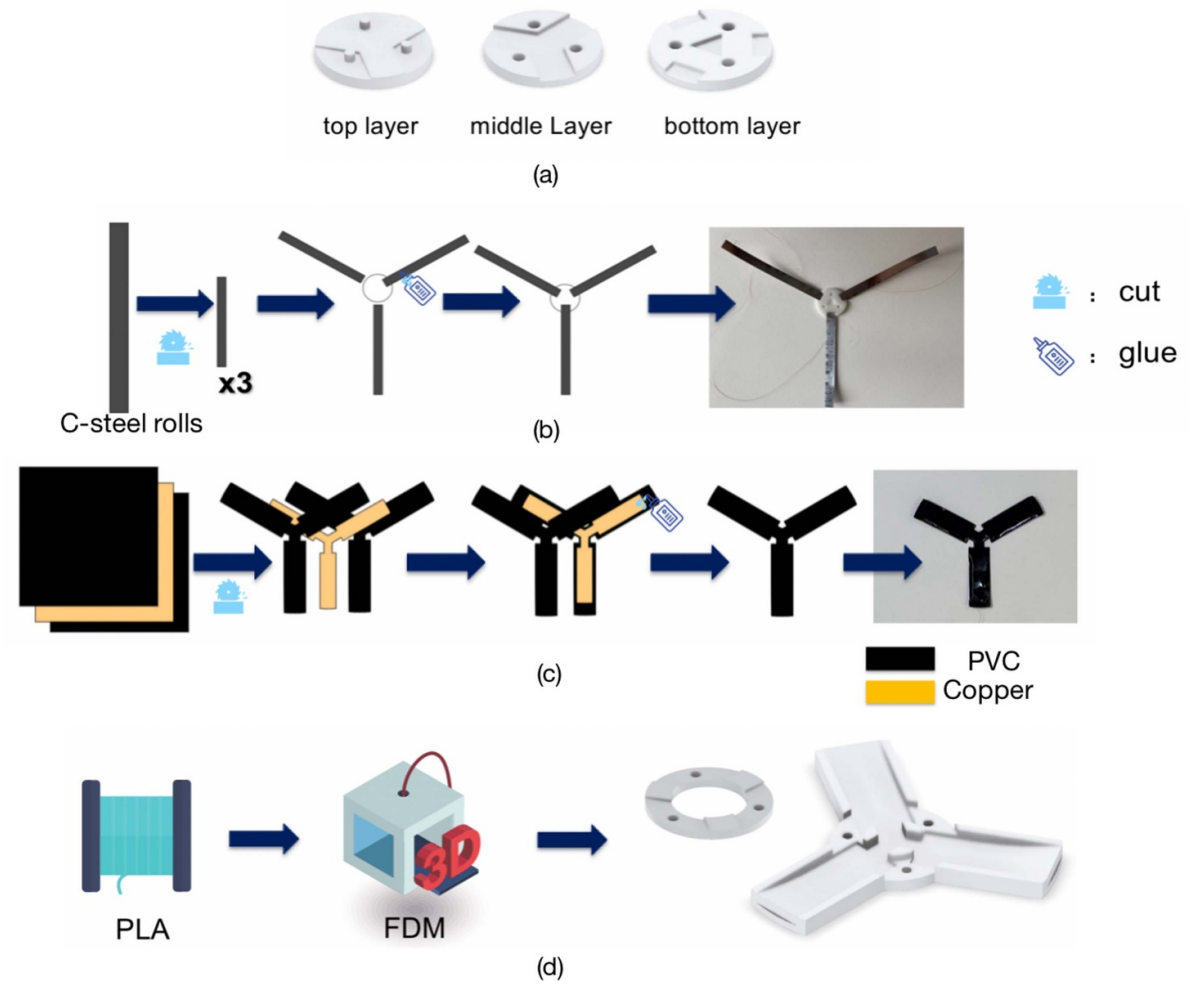

Figure 4. Schematic diagram of (a) three layers of the contact panel, (b) fabrication of movable electrodes, (c) fabrication of fixed electrode, and (d) fabrication of fixing ring and curved base.

through the inextensible string. The output force of the haptic device, when actuated, is obtained directly by recording the reading of the force sensor.

(3) **Power output and energy conversion efficiency**: In order to measure the power output of the 3D-ElectroZip Touch, it was assumed that the power output of the 3D-ElectroZip Touch is equal to the rate of change of the spring's elastic potential energy until the device reaches the equilibrium state. The equation to calculate the average power can be summarized as:

$$P_{\text{3D - ETouch}} = \frac{\Delta E}{t} = \frac{k \cdot \Delta x^2}{2t} = \frac{k \cdot \sum_{i=0}^{t+1} (x_{i+1} - x_i)^2}{2t} \quad (1)$$

where $P_{\text{3D - ETouch}}$ is the average power of the 3D-ElectroZip Touch, ΔE is the change in elastic potential energy, k is the spring stiffness, t is the time taken to reach equilibrium state, and x_i is the displacement at time point i and was taken every 0.001 s.

The power transfer efficiency is calculated as the ratio of the average power and total electric power of all channels:

$$\eta = \frac{P_{\text{3D - ETouch}}}{P_{\text{E}}} = \frac{P_{\text{3D - ETouch}}}{\sum_{j=1}^{4} V_j I_j} \quad (2)$$

where η is power transfer efficiency, P_{E} is electric power, V_j is voltage applied by power channel j, and I_j is the current generated in the electrode connected to channel j.

4. Results

Figure 6 shows the device's positions at 0.4 s intervals across three distinct modes of motion (diagonal, normal, and vertical). This section describes the performance analysis of the 3D-ElectroZip Touch, considering displacement, force generation, power output, and energy transfer efficiency. All measurements were conducted under four varying input voltages, ranging from 6 kV to 9 kV, with a 1 kV increment.

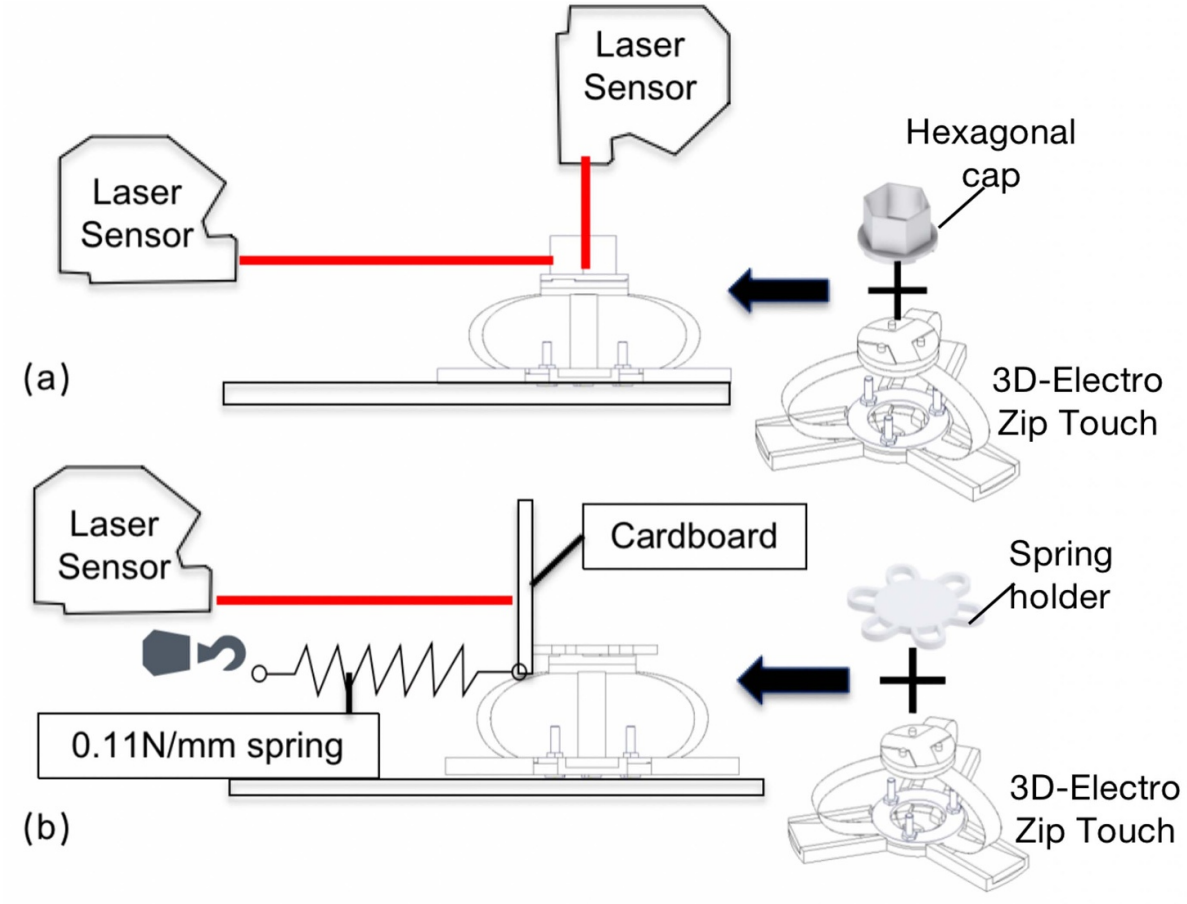

Figure 5. Measurement setup schematics for (a) displacement and (b) force.

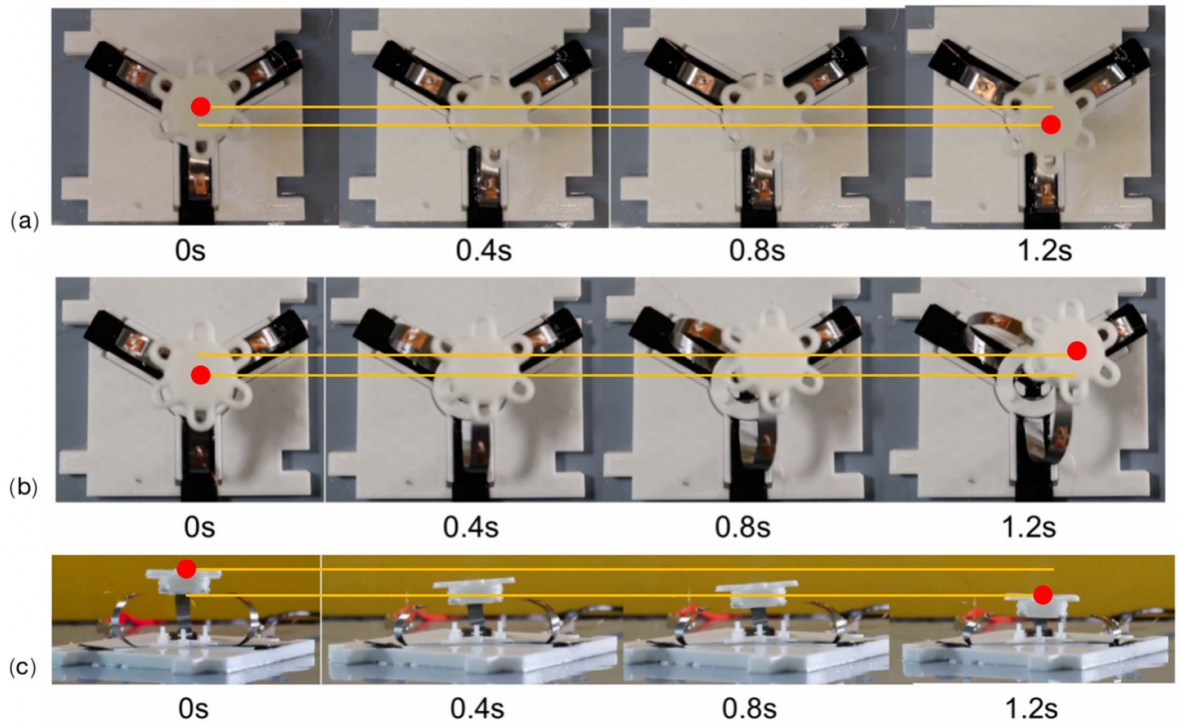

Figure 6. Screenshots of (a) diagonal, (b) normal, and (c) vertical motions every 0.4 s at 6 kV. Red dot and yellow lines indicate displacements of the contact panel.

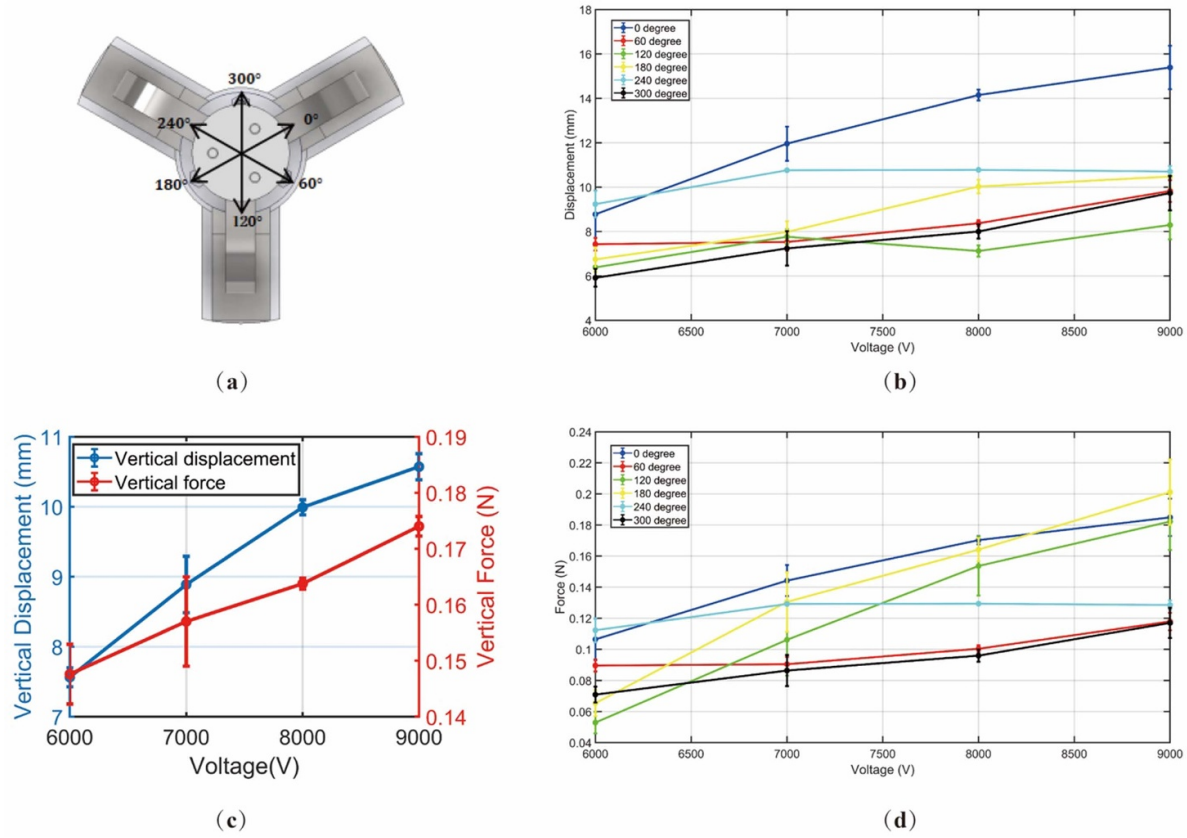

Figure 7. (a) Six angles measured for diagonal motion of the haptic device; (b) displacement of the haptic device for various horizontal motions under different voltage; (c) vertical force and displacement, and (d) generated force of the haptic device under different voltages for horizontal motions. The error bars indicate standard deviations of multiple trials under corresponding voltages.

4.1. Displacement and force

Figure 7 shows the results of maximum displacement and generated force at four different voltages for both the vertical and six horizontal directions as detailed in figure 7(a). Generally, an increase in voltages corelated with higher displacement and force. The variations observed in generated force and displacement across different directions can be attributed to fabrication and assembly inconsistencies. While these discrepancies should generally be insignificant in a symmetric structure between tests at 0, 120, and 240 degrees, as well as between 60, 180 and 300 degrees, potential imperfections in manual assembly, such as the imprecise cuts and curvature of each arc, along with the top contact panel not being perfectly centered, can lead to minor variations in mechanical resistance when pulled in various directions by the DLZ force. This, in turn, results in slight variations in displacement and force measurements across various directions. Examples include higher displacement at 0 degrees and larger error bars at specific voltages. The presence of dielectric liquid at the zipping point also plays a key role in the functionality of the haptic device. The dielectric liquid moves along the zipping ribbons, drawn into the high electric field zipping point by the dielectrophoretic force. Random deterioration of the liquid could cause a decrease in force, as seen in cases like minor decrease in displacement at 120 degrees 8 kV, and smaller changes in force with voltage increases, such as 240 degrees at 7 and 8 kV. However, these discrepancies do not impact the overall performance and actuation behavior of the 3D-Electro Zip Touch. The maximum displacement generated by the 3D-ElectroZip Touch is able to contract the device by more than 70%, calculated by dividing the displacement of the 3D-ElectroZip Touch by the distance between the bottom of the contact panel and the base, which is about 15 mm on average.

4.2. Power and energy

Results of average power and energy conversion efficiency are shown in figure 8. Average power for both directions peaks at 9 kV. The maximal power in the diagonal direction is 0.075 W, and the maximal power in the normal direction is 0.038 W. Energy efficiencies of normal and diagonal motion peak at 7 kV (68%) and 8 kV (72%), respectively, and both drop to their minimum (around only 20%) at 9 kV. This substantial efficiency decline is attributed to current leakage through the

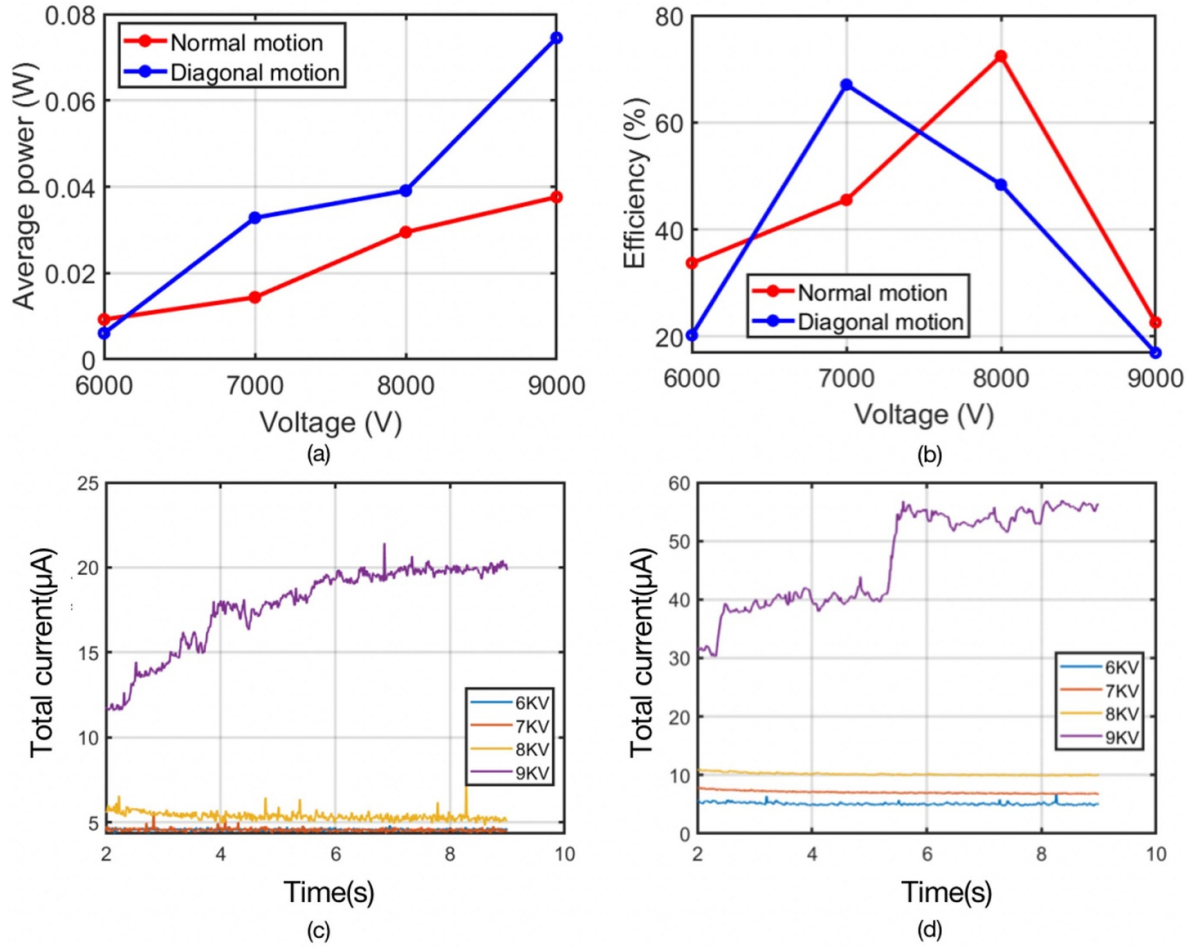

Figure 8. (a) Average mechanical power and (b) efficiency of the 3D-ElectroZip Touch at different voltages. (c) The total current flowing through the 3D-ElectroZip Touch during normal motion under different voltages. (d) The total current flowing through the 3D-ElectroZip Touch during diagonal motion under different voltages.

insulator at higher voltages. As shown in figures 8(c) and (d), the total current in the electrodes at 9 kV is five times higher than at 8 kV, resulting in reduced efficiency at the higher voltage.

5. Discussion

5.1. Performance evaluation

The developed haptic technology can be controlled to achieve multi-directional motion with a minimal displacement of at least 5 mm, which is far beyond the minimum displacement (2 μm to 20 μm) that skin can detect. The generated force also falls in the range of sensitivity of the skin, beyond the minimum detectable force by the skin (50 mN) [33]. The device, therefore, can deliver distinguishable sensations across its seven different motion modes, but user trials would be needed to determine its sensitivity, particularly once the structure is miniaturized.

The 3D-ElectroZip Touch swiftly responds to input voltage fluctuations. Figure 9 displays the average time the device takes to reach its maximum displacement (complete actuation) and the 63.2% of its maximum displacement for different voltage levels. We found that the time required for complete device actuation reduces from 1.5 s to 0.5 s as applied voltages increases from 6 kV to 9 kV. In contrast, the devices exhibit a faster response time, reaching 63.2% of the maximum displacement nearly as quickly as the average human body's response time (0.2 s) [34]. The slight variations in the response time across different voltages can be attributed to the minor differences in the initial resting position of the haptic device's contact tip before each test or the random distribution of the liquid dielectric (silicone oil) as it is drawn towards the zipping point via dielectrophoretic forces at the beginning of each test. The displacement during this short actuation is still noticeable by human skin, with average readings of 7.3203, 9.1456, 9.6162, 10.3172 mm for normal motion and 6.0279, 6.8257, 7.9208, 9.0104 mm for diagonal motion, at voltages ranging from 6 kV to 9 kV. Although a gradual zipping mechanism drives the actuation, its initial movement, occurring within a very short time, recorded at the initial 10% actuation time (0.07 ± 0.003 s), is sufficient to provide noticeable feedback to human skin. The average readings for normal motion are

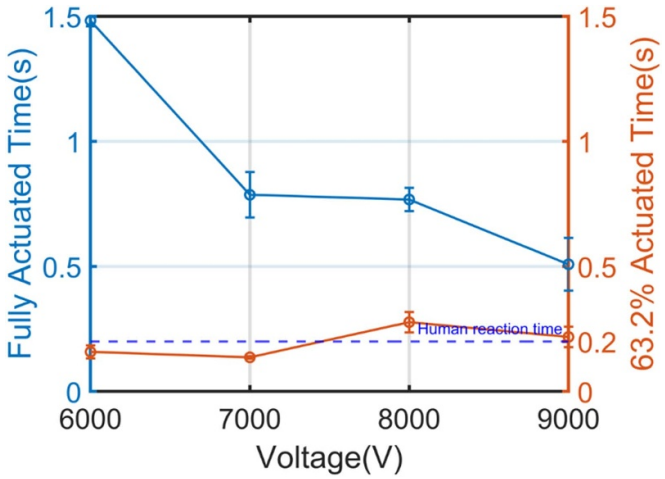

Figure 9. Time taken for the device to reach its maximum displacement and 63.2% of it at different voltages, with the human average reaction time indicated by a dashed line.

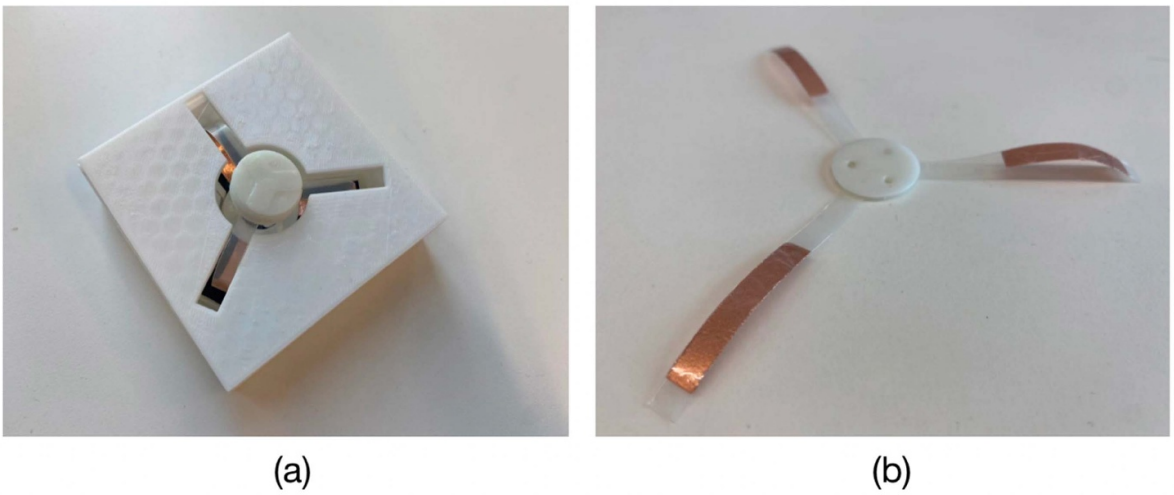

Figure 10. (a) The 3D-ElectroZip Touch encapsulated in a 3D-printed plastic box. (b) Top movable electrodes fabricated using polyethylene terephthalate and copper tape.

1.01 ± 0.15 mm and for diagonal motion, 0.89 ± 0.15 mm, with voltage ranging from 6 kV to 9 kV.

5.2. Potential enhancement

The developed proof-of-concept technology exhibits a lightweight and compliant device capable of quick, multi-directional motion. Preliminary characterization confirms its potential for haptic device applications. However, to conduct user experiments, the technology needs further advancements. Encapsulating the device in a plastic box as shown in figure 10(a) primarily reduce the risk of direct contact between high-voltage electronics and the user. It, however, limits the movement of the haptic device to only three horizontal directions. To fully isolate the conductive parts from the contact panel, since only a small part of the top electrode contributes to the electrostatic zipping, the top half of the bending electrodes can also be replaced with a non-conductive material as shown in (figure 10(b)). Using a material with an identical mechanical stiffness to that of the 0.03 mm stainless steel to replace this ribbon will ensure achieving a similar performance.

Our future work on this technology will include scaling it down to develop a dense array of haptic interfaces. Such small and compliant haptic units can be incorporated in wearables, allowing for advanced haptic interface for human–machine interaction to communicate complex information, exploiting multifunctional capabilities of the device.

6. Conclusion

In summary, a multi-directional force feedback device has been developed using DLZ actuation concept. 3D-ElectroZip Touch is capable of moving in vertical and multiple horizontal directions to stimulate the sense of normal and shear forces. Its performance in terms of displacement, force and actuation time has been quantified. This proof-of-concept DLZ-based

electrostatic haptic device serves as a stepping stone towards the development of a miniaturized array of haptic units for use in tactile display and wearables. Such arrays would have the capability to convey complex information to the user in different directions and intensities.

Data availability statement

The data that support the findings of this study are openly available at the following URL/DOI: https://doi.org/10.5281/zenodo.12751985.

Acknowledgments

M T acknowledges Imperial College Bioengineering Fellowship and W S was supported by the Natural Science Foundation of Shannxi Province of China (No. 2024JC-YBQN-0028) and China Scholarship Council (No. 202108610144).

ORCID iD

Yuhan Pan https://orcid.org/0000-0001-5744-8496

References

[1] Biswas S and Visell Y 2019 Emerging material technologies for haptics *Adv. Mater. Technol.* **4** 1900042
[2] Chen D, Song A, Tian L, Ouyang Q and Xiong P 2019 Development of a multidirectional controlled small-scale spherical MR actuator for haptic applications *IEEE/ASME Trans. Mechatronics* **24** 1597–607
[3] Burdea G C 1996 *Force and Touch Feedback for Virtual Reality* (John Wiley & Sons, Inc.)
[4] Hayward V, Astley O R, Cruz-Hernandez M, Grant D and Robles-De-La-Torre G 2004 Haptic interfaces and devices *Sens. Rev.* **24** 16–29
[5] Coles T R, Meglan D and John N W 2010 The role of haptics in medical training simulators: a survey of the state of the art *IEEE Trans. Haptics* **4** 51–66
[6] Okamura A M 2009 Haptic feedback in robot-assisted minimally invasive surgery *Curr. Opin. Urol.* **19** 102
[7] Morash V S, Russomanno A, Gillespie R B and O'Modhrain S 2017 Evaluating approaches to rendering braille text on a high-density pin display *IEEE Trans. Haptics* **11** 476–81
[8] Miriyev A, Stack K and Lipson H 2017 Soft material for soft actuators *Nat. Commun.* **8** 596
[9] Wu X, Kim S-H, Zhu H, Ji C-H and Allen M G 2012 A refreshable braille cell based on pneumatic microbubble actuators *J. Microelectromech. Syst.* **21** 908–16
[10] Agharese N *et al* 2018 HapWRAP: soft growing wearable haptic device *2018 IEEE Int. Conf. on Robotics and Automation (ICRA)* (IEEE) pp 5466–72
[11] Miruchna V, Walter R, Lindlbauer D, Lehmann M, Von Klitzing R and Müller J 2015 Geltouch: localized tactile feedback through thin, programmable gel *Proc. 28th Annual ACM Symp. on User Interface Software & Technology* pp 3–10
[12] Zhao Y *et al* 2023 Ultra-stretchable hydrogel thermocouples for intelligent wearables *Sci. China Mater.* **66** 1934–40
[13] Zhang G, Furusho J and Sakaguchi M 2000 Vibration suppression control of robot arms using a homogeneous-type electrorheological fluid *IEEE/ASME Trans. Mechatronics* **5** 302–9
[14] Blake J and Gurocak H B 2009 Haptic glove with MR brakes for virtual reality *IEEE/ASME Trans. Mechatronics* **14** 606–15
[15] Yin X, Wu C, Wen S and Zhang J 2021 Smart design of Z-width expanded thumb haptic interface using magnetorheological fluids *IEEE Trans. Instrum. Meas.* **70** 1–11
[16] Heo Y H, Choi D-S, Yun I-H and Kim S-Y 2020 A tiny haptic knob based on magnetorheological fluids *Appl. Sci.* **10** 5118
[17] Chen J, Teo E H T and Yao K 2023 Electromechanical actuators for haptic feedback with fingertip contact *Actuators* **12** 104
[18] Korres G, Park W and Eid M 2021 Contactless kinesthetic feedback to support handwriting using magnetic force *IEEE Trans. Haptics* **14** 825–34
[19] Zárate J J and Shea H 2016 Using pot-magnets to enable stable and scalable electromagnetic tactile displays *IEEE Trans. Haptics* **10** 106–12
[20] Kastor N, Dandu B, Bassari V, Reardon G and Visell Y 2023 Ferrofluid electromagnetic actuators for high-fidelity haptic feedback *Sens. Actuators* A **355** 114252
[21] Guo Y, Tong Q, Zhao P, Zhang Y and Wang D 2022 Electromagnetic-actuated soft tactile device using a pull-push latch structure *IEEE Trans. Ind. Electron.* **70** 10344–52
[22] Kim J, Han B-K, Pyo D, Ryu S, Kim H and Kwon D-S 2020 Braille display for portable device using flip-latch structured electromagnetic actuator *IEEE Trans. Haptics* **13** 59–65
[23] Hosseini M, Sengül A, Pane Y, De Schutter J and Bruyninck H 2018 Exoten-glove: a force-feedback haptic glove based on twisted string actuation system *2018 27th IEEE Int. Symp. on Robot and Human Interactive Communication (RO-MAN)* (IEEE) p 320–7
[24] Amirpour E *et al* 2019 Design and optimization of a multi-DOF hand exoskeleton for haptic applications *2019 7th Int. Conf. on Robotics and Mechatronics (Icrom)* (IEEE) pp 270–5
[25] Oh J-S, Sohn J W and Choi S-B 2022 Applications of magnetorheological fluid actuator to multi-DOF systems: state-of-the-art from 2015 to 2021 *Actuators* **11** 44
[26] Giri G S, Maddahi Y and Zareinia K 2021 An application-based review of haptics technology *Robotics* **10** 29
[27] Mintchev S, Salerno M, Cherpillod A, Scaduto S and Paik J 2019 A portable three-degrees-of-freedom force feedback origami robot for human–robot interactions *Nat. Mach. Intell.* **1** 584–93
[28] Zhao H, Hussain A M, Israr A, Vogt D M, Duduta M, Clarke D R and Wood R J 2020 A wearable soft haptic communicator based on dielectric elastomer actuators *Soft Robot.* **7** 451–61
[29] Leroy E, Hinchet R and Shea H 2020 Multimode hydraulically amplified electrostatic actuators for wearable haptics *Adv. Mater.* **32** 2002564
[30] Kim U *et al* 2013 A transparent and stretchable graphene-based actuator for tactile display *Nanotechnology* **24** 145501
[31] Hau S, York A and Seelecke S 2016 High-force dielectric electroactive polymer (DEAP) membrane actuator *Proc. SPIE* **9798** 21–27
[32] Taghavi M, Helps T and Rossiter J 2018 Electro-ribbon actuators and electro-origami robots *Sci. Robot.* **3** eaau9795
[33] King H H, Donlin R and Hannaford B 2010 Perceptual thresholds for single vs. multi-finger haptic interaction *2010 IEEE Haptics Symp.* (IEEE) pp 95–99
[34] Wang H, Adamzadeh M, Burgei W A, Foley S E and Zhou H 2022 Extracting human reaction time from observations in the method of constant stimuli *J. Appl. Math. Phys.* **10** 3316–45